BNL-102165-2014-TECH
RHIC/AP/56;BNL-102165-2013-IR

Linear Coupling Effect of the Helical Snakes and Rotators in RHIC

F. Pilat

February 1995

Collider Accelerator Department
Brookhaven National Laboratory

U.S. Department of Energy
USDOE Office of Science (SC)

DISCLAIMER

RHIC/AP/56

February 1995

Linear Coupling effect of the Helical Snakes and Rotators in RHIC

F. Pilat

1. Introduction

The following note describes a simple way to calculate the linear coupling effect of helical snakes and rotators in RHIC by calculating the minimum tune separation (ΔQ_{min}) from the one-turn linear map[1]. The latter is derived by using a strictly linear model: the snakes and rotators are represented by matrices and the RHIC lattice by the transfer matrices between the location of the snakes and rotators. The snake matrix obtained by numerical integration of an ensemble of trajectories [2] is compared to the map for the same helical fields derived by differential algebra techniques. [3] The matrices obtained numerically are also compared to the matrices for helical fields calculated analytically by simplification of the equations of motions in the snake [4]. The respective coupling effects are evaluated. The linear coupling generated in RHIC by the Siberian snakes and spin rotators seems well within the capability of the decoupling correction system at injection, and negligible at storage energy.
This Note updates and completes the already published RAP Note 44.

2. The present snake and rotator design

The present nominal design for the RHIC helical snake [5] consists of 4 modules of 2.4 m length, where the helix wavelength equals the module length (see scheme in Figure 1). The B_0 field for the outer modules is 1.458 T and for the inner ones 4 T, a configuration that minimizes the closed orbit excursions in the snake ($\Delta y < 27$ mm at the injection γ of 27).
Two snakes will be installed in each RHIC ring at locations separated in betatron phase by πQ_x and πQ_y (The nominal tunes for RHIC are $Q_x = 28.19$ and $Q_y = 29.18$) next to the Q7 quadrupoles in the 10 o'clock and 4 o'clock interaction regions.
The present nominal design of the spin rotators is described in [6] and further optimizations based on this selected design have been presented [7]. Similarly to the snake, it consists of 4 modules of 2.4 m length and helix wavelength. The fields, schematically shown in Figure 2, have different magnitude on axis, orientation and helicity, in order to achieve a longitudinal polarization at the experimental interaction points. The main conceptual differences from the snake in the rotator design are that the amount of spin rotation required varies with energy and that the field integral of the fringe fields does not cancel by symmetry over the 4 rotator modules, a nice symmetry property of the Siberian snake.
2 spin rotators per interaction region and per beam are necessary to longitudinally polarize the

proton beam in the 6 o'clock and 8 o'clock interaction points and to restore the vertical polarization downstream. The rotators are located symmetrically around the 6 o'clock and 8 o'clock IPs, in the long drifts between the Q3 and Q4 quadrupoles. The location, slot length and schematic design of snakes and rotators are represented in the RHIC lattice database RHIC92.0.5.

Figure 1. Schematic view of the RHIC helical snake.

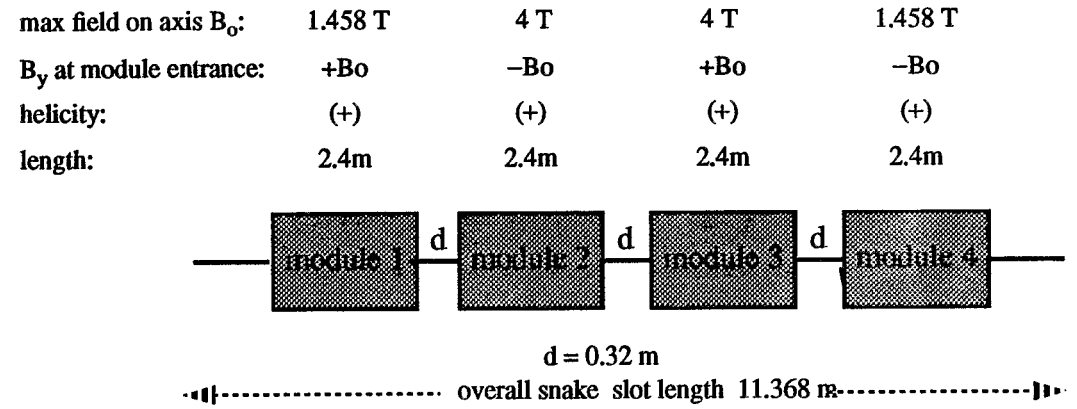

Figure 2. Schematic view of the RHIC helical spin rotator.

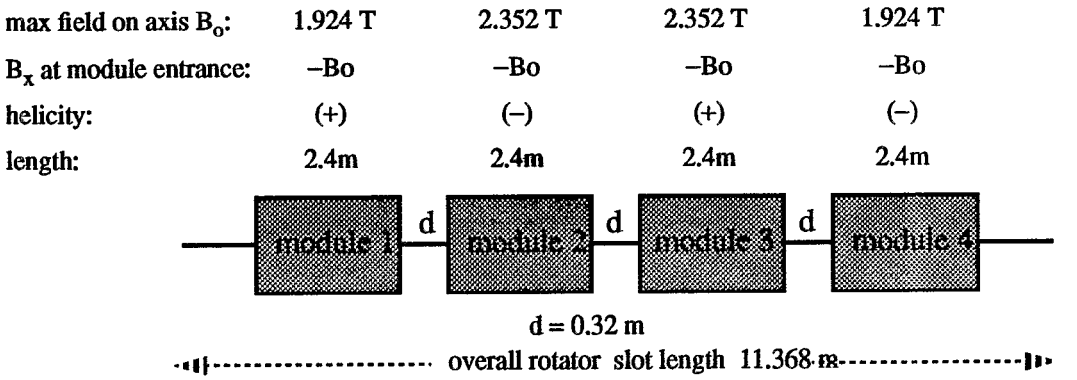

3. The snake matrix

3.1 Numerical approach (SNIG)

The SNIG program [2], which is being used for snake design and optimization, allows the computation of particle trajectories in the snake by integrating the equations of motion in the magnetic field of the snake. The helical field is expressed analytically as a continuous superposition of wigglers, an expression which has the right symmetry and satisfies Maxwell equations. A third order expansion of this field proved accurate enough for trajectory calculations. For a detailed discussion of the field and equations of motion in the helical snake see [8][9][10]. The SNIG program has been extended to allow the derivation of first and second order transfer matrices from the integration of particle trajectories [5]. A distribution of particles is randomly generated in an ellipse, whose parameters are defined by user-specified Twiss functions and emittances at the entrance of

```
BEAM

-13.593543< xo[mm] <   13.836684 *    -1.357523< uo[mrad] <    1.383668
-13.660439< yo[mm] <   13.976768 *    -1.398677< vo[mrad] <    1.368125

MATRIX

[ x ]       [   -1.052     ]       [    1.055       12.30     -1.2262E-02  5.5537E-02 ]       [ xo ]
[   ]       [              ]       [                                                 ]       [    ]
[ u ]       [ -4.6343E-03  ]       [   9.1681E-03   1.055     -2.1174E-05  2.1419E-02 ]       [ uo ]
[   ]   =   [              ]   +   [                                                 ]   X   [    ]
[ y ]       [   3.0430E-02 ]       [   4.8444E-03 -5.6812E-02   1.019       12.10     ]       [ yo ]
[   ]       [              ]       [                                                 ]       [    ]
[ v ]       [   5.5211E-03 ]       [ -5.7644E-05 -1.4654E-02  3.1978E-03   1.019     ]       [ vo ]

        [   3.679E-07 -1.121E-05 -2.136E-07 -4.337E-05 -2.884E-04 -4.265E-05 -2.580E-04 -2.906E-06 -6.720E-06 -6.680E-04 ]
        [                                                                                                               ]
        [  -5.338E-08 -2.905E-06  9.274E-09 -7.125E-08 -1.752E-05 -1.226E-07  3.967E-05 -1.332E-08  4.975E-06  2.717E-05 ]
  +     [                                                                                                               ]
        [   2.586E-06  1.664E-04  3.521E-06  7.294E-06  5.385E-04 -6.579E-06  3.989E-04  1.477E-06  6.248E-05  1.898E-04 ]
        [                                                                                                               ]
        [   3.269E-07  3.627E-06 -5.511E-08 -3.314E-06 -5.017E-05 -4.897E-06 -4.775E-05  2.395E-07  2.762E-06 -1.467E-05 ]

  X     [      xo**2       xo*uo       xo*yo       xo*vo       uo**2       uo*yo       uo*vo       yo**2       yo*vo       vo**2   ]

ERRORS

            [   3.3652E-07 ]       [   1.5414E-07  2.0716E-06  9.6325E-08  9.4605E-07 ]
            [              ]       [                                                  ]
            [   2.2915E-08 ]       [   1.0162E-08  1.3494E-07  6.6639E-09  7.4240E-08 ]
            [              ]       [                                                  ]
            [   3.3685E-07 ]       [   1.3858E-07  1.9557E-06  9.0640E-08  1.0662E-06 ]
            [              ]       [                                                  ]
            [   1.4042E-08 ]       [   7.3773E-09  1.0709E-07  4.0524E-09  4.2147E-08 ]

        [   8.461E-09  2.233E-08  1.067E-08  9.935E-08  6.040E-07  1.230E-07  1.142E-06  4.059E-09  1.340E-07  1.754E-07 ]
        [                                                                                                               ]
        [   7.889E-10  1.836E-09  7.909E-10  9.454E-09  4.343E-08  8.749E-09  9.210E-08  3.665E-10  1.234E-08  1.197E-08 ]
        [                                                                                                               ]
        [   9.964E-09  2.552E-08  1.132E-08  1.218E-07  6.678E-07  1.252E-07  1.196E-06  4.913E-09  1.589E-07  8.938E-08 ]
        [                                                                                                               ]
        [   1.760E-10  6.504E-10  4.993E-10  2.032E-09  2.371E-08  5.435E-09  3.811E-08  1.414E-10  2.354E-09  5.565E-09 ]

SPIN

start spin:          0.000000000  1.000000000  0.000000000
final spin:         -0.082344043 -0.993497064 -0.078449434
with dispersion:     3.4104E-03   1.7186E-04   4.1319E-03
axis angles:            136.037       -0.020
with dispersion:     0.1650       0.1459
```

Figure 3. First and second order matrices for the helical snake at $\gamma = 27$ (injection)

Date: Feb 9 1995 15:44:05

```
BEAM

-13.593543< xo[mm] <   13.836684 *    -1.357523< uo[mrad] <    1.383668
-13.660439< yo[mm] <   13.976768 *    -1.398677< vo[mrad] <    1.368125

MATRIX

[ x ]        [  -0.1256     ]        [    1.001       12.00     -1.2293E-04  5.6093E-04 ]        [ xo ]
[   ]        [              ]        [                                                 ]        [    ]
[ u ]        [  -5.7666E-06 ]        [   9.1816E-05   1.001     -1.1994E-09  2.1638E-04 ]        [ uo ]
[   ]   =    [              ]   +    [                                                 ]   X    [    ]
[ y ]        [   3.3421E-05 ]        [   5.1947E-05 -5.6179E-04   1.000       12.00     ]        [ yo ]
[   ]        [              ]        [                                                 ]        [    ]
[ v ]        [   6.1165E-06 ]        [  -5.9746E-09 -1.4548E-04  3.1998E-05   1.000     ]        [ vo ]

        [ -1.058E-07 -1.402E-08 -4.550E-12 -3.430E-06 -1.800E-05 -3.750E-06 -2.256E-05 -3.232E-07 -1.213E-08 -5.887E-05 ]
        [                                                                                                             ]
        [ -3.207E-11  2.104E-07  1.296E-10  1.049E-10  1.258E-06  1.277E-09  3.431E-06 -2.508E-12  6.460E-07  3.869E-06 ]
  +     [                                                                                                             ]
        [  3.440E-09  1.099E-05  2.169E-07  9.951E-09  3.393E-05 -6.974E-09  4.088E-05  1.380E-09  3.771E-06  1.132E-05 ]
        [                                                                                                             ]
        [  3.605E-10  3.705E-09 -4.076E-11 -2.168E-07 -5.301E-06 -2.183E-07 -2.613E-06  2.529E-10  2.906E-09 -1.875E-06 ]

  X     [     xo**2      xo*uo      xo*yo      xo*vo      uo**2      uo*yo      uo*vo      yo**2      yo*vo      vo**2  ]

ERRORS

             [   1.3295E-07 ]        [   6.9893E-08  8.5963E-07  3.4320E-08  4.0736E-07 ]
             [              ]        [                                                  ]
             [   7.0600E-09 ]        [   3.4329E-09  4.4703E-08  1.9428E-09  1.8155E-08 ]
             [              ]        [                                                  ]
             [   5.6442E-08 ]        [   2.4782E-08  3.1838E-07  2.5810E-08  2.3842E-07 ]
             [              ]        [                                                  ]
             [   5.2843E-09 ]        [   2.6992E-09  3.3282E-08  1.4204E-09  2.1073E-08 ]

        [  2.127E-09  1.017E-08  4.611E-09  2.546E-08  2.544E-07  5.002E-08  3.894E-07  1.177E-09  4.182E-08  6.763E-08 ]
        [                                                                                                             ]
        [  5.088E-11  5.053E-10  2.217E-10  6.141E-10  1.566E-08  2.665E-09  1.972E-08  5.019E-11  1.371E-09  3.741E-09 ]
        [                                                                                                             ]
        [  1.724E-09  5.238E-09  1.892E-09  1.835E-08  1.393E-07  2.318E-08  2.046E-07  8.112E-10  2.496E-08  3.129E-08 ]
        [                                                                                                             ]
        [  1.645E-10  4.983E-10  1.784E-10  1.903E-09  8.168E-09  1.823E-09  1.833E-08  7.262E-11  2.584E-09  3.552E-09 ]

 SPIN

start spin:          0.000000000  1.000000000  0.000000000
final spin:         -0.074970638 -0.994664549 -0.070851527
with dispersion:     9.7227E-04   8.4779E-05   9.7292E-04
axis angles:           136.590       -0.001
with dispersion:     5.8593E-02   3.2413E-02
```

Figure 4. First and second order matrices for the helical snake at $\gamma = 268$ (storage)

the snake. The initial conditions, typically 50 to 100, are tracked through the snake with SNIG and a polynomial fit of the dependence of final from initial conditions is performed. That allows one to derive first and second order transverse matrices, as well as the statistical errors associated. A typical result for the present snake design at injection (γ=27) is listed in Figure 3.
The dependence of the numerical matrix on input parameters, as *number of particles* tracked, *shape* and *size* of the initial *ellipse*, random *seed*, *offset of the ellipse center* (closed orbit at the snake entrance), and *energy* has been systematically checked. The fit results proved to be insensitive (variation of matrix terms < 1%) to most of the parameters varied, with the exception of the ellipse offset and energy. However, in order to have appreciable effects on the matrix (>>1%) the ellipse center offset has to be ~3cm, an unrealistic value for the closed orbit at the entrance of the snake in a corrected machine. The matrix obviously changes with energy. Results for the design snake at storage energy (γ=268) are listed in Figure 4. At higher γ the diagonal terms are ~1, the length ~12m and focusing and coupling terms of the linear matrix as expected decrease with energy.

3.2 The truncated Taylor map approach (PAC++)

A method has recently been developed [3] that allows the computation of arbitrary order truncated Taylor maps for non-standard accelerator elements such as a helical field. The method uses a Runge-Kutta integrator for the magnetic field in the framework of the general purpose PAC++ Differential Algebra package which calculates the Taylor map of the element to the desired order. The representation used for the helical dipole field is described in [10] and the map extraction program (HELIX) is accessible in the public area of the RHIC Unix Domain[11].
If we limit the map to second order we can directly compare the map result to the matrices obtained numerically by SNIG. The model for the fringe fields is different in the present implementation of SNIG and the map package. SNIG assumes a helical fringe field which decays longitudinally over a distance equal to half of the dipole aperture, while the PAC++ map approximates the fringe field with thin multipoles at the entrance and exit of the helical module. A comparison between SNIG and PAC++ for one helical module where the fringe fields are set to zero in both cases (see Figure 5) shows excellent agreement between the two approaches.
The truncated Taylor map technique allows furthermore an evaluation of snake and rotator effects to higher orders, and opens the possibility to describe helical fields (or other non standard elements) in TEAPOT and other general purpose codes.

3.3 Analytical approach

It is possible to derive a first order transfer matrix for 1 module of the helical snake by expanding around the reference helical orbit, approximating the helical dipole field and simplifying the equations of motion by averaging sin-like and cosine-like terms. For a detailed discussion of the derivation see [3].
I will only repeat here the final form of the matrix, for a helical field where $L = \lambda = 2\pi/k$, with λ

```
****************************************** SNIG ************************************************************

                zero order terms[mm]     first order terms

  [ x ]         [   4.8695E-03 ]         [   0.9996       2.400      -3.0760E-04 -8.2046E-04 ]         [ xo ]
  [   ]         [              ]         [                                                   ]         [    ]
  [ u ]         [   2.0305E-03 ]         [ -1.7920E-04    1.000      -1.7083E-07 -2.3977E-04 ]         [ uo ]
  [   ]    =    [              ]    +    [                                                   ]    X    [    ]
  [ y ]         [   -15.83     ]         [   2.3913E-04  4.9206E-04  0.9996       2.400     ]         [ yo ]
  [   ]         [              ]         [                                                   ]         [    ]
  [ v ]         [   4.2507E-03 ]         [ -2.4291E-08  3.0787E-04 -5.3702E-04  0.9991     ]         [ vo ]

   second order terms

  [   3.209E-08  2.076E-05  2.714E-05  5.565E-08  1.242E-05  4.941E-09 -7.758E-06  1.434E-08  2.076E-05  3.722E-05
  [
  [   1.838E-08  2.961E-08  2.671E-08 -2.707E-05 -1.035E-05 -2.708E-05 -6.498E-05  1.486E-08  6.500E-08  1.046E-05
  [
  [  -4.069E-05 -2.901E-09  1.413E-08 -2.059E-05 -4.153E-06  2.074E-05 -2.465E-05 -1.355E-05 -9.675E-08 -1.291E-05
  [
  [   8.681E-09  8.135E-05  1.931E-09 -7.650E-09  9.765E-05 -4.656E-08 -2.075E-05  2.549E-08  2.721E-05  3.261E-05

X [      xo**2       xo*uo       xo*yo       xo*vo       uo**2       uo*yo       uo*vo       yo**2       yo*vo       vo**2

************************************ PAC++ DA MAP ******************************************************

ZMap : order = 2 dimension = 4

    1  4.867688e-06  2.028987e-06 -1.582709e-02  4.249112e-06   0  0  0  0       zero order terms [m]

    2  9.995705e-01 -1.791592e-04  2.390698e-04 -2.461688e-08   1  0  0  0       first order terms
    3  2.399748e+00  9.999995e-01  4.919867e-04  3.077879e-04   0  1  0  0
    4 -3.075189e-04 -1.709400e-07  9.995705e-01 -5.368832e-04   0  0  1  0
    5 -8.203133e-04 -2.396907e-04  2.399774e+00  9.991407e-01   0  0  0  1

    6  3.197996e-05  1.835364e-05 -4.068019e-02  8.507707e-06   2  0  0  0       second order terms
    7  2.075559e-02  2.966097e-05 -4.213836e-06  8.134410e-02   1  1  0  0
    8  2.713356e-02  2.668582e-05  1.391044e-05  1.950271e-06   1  0  1  0
    9  5.455311e-05 -2.706018e-02 -2.071930e-02 -3.661227e-06   1  0  0  1
   10  1.246628e-02 -1.034777e-02 -3.957300e-03  9.764139e-02   0  2  0  0
   11  4.260976e-06 -2.708114e-02  2.071650e-02 -4.632747e-05   0  1  1  0
   12 -7.863063e-03 -6.500733e-02 -2.488950e-02 -2.081212e-02   0  1  0  1
   13  1.435950e-05  1.485362e-05 -1.354683e-02  2.548836e-05   0  0  2  0
   14  2.076176e-02  6.481591e-05  5.531478e-05  2.720437e-02   0  0  1  1
   15  3.736369e-02  1.044931e-02 -1.181793e-02  3.264057e-02   0  0  0  2
```

Figure 5. Comparison of SNIG matrices and PAC++ map to second order for a helical dipole module (no fringe fields).

Date:

and k respectively wave length and wave number of the helix.

$$\begin{bmatrix} \cos(\delta L) & 0 & -\sin(\delta L) & 0 \\ 0 & \cos(\delta L) & 0 & -\sin(\delta L) \\ \sin(\delta L) & 0 & \cos(\delta L) & 0 \\ 0 & \sin(\delta L) & 0 & \cos(\delta L) \end{bmatrix}$$

$$\begin{bmatrix} \cos(\lambda_o L) & \frac{\sin(\lambda_o L)}{\lambda_o} & 0 & 0 \\ -\lambda_o \sin(\lambda_o L) & \cos(\lambda_o L) & 0 & 0 \\ 0 & 0 & \cos(\lambda_o L) & \frac{\sin(\lambda_o L)}{\lambda_o} \\ 0 & 0 & -\lambda_o \sin(\lambda_o L) & \cos(\lambda_o L) \end{bmatrix}$$

where $\delta = 1/(2k\rho^2)$, $\lambda_o = \sqrt{\varepsilon^2 + \delta^2}$ where $\varepsilon^2 = 1/(2\rho^2)$ and $\rho = (B\rho)/B_o$.

For the snake design at the injection γ of 27 the matrices for the 1.458 T and the 4 T modules are respectively :

M1

$$\begin{bmatrix} 0.9996 & 2.3996 & -0.00014 & -0.00033 \\ -0.00035 & 0.9996 & 0.00000 & -0.00014 \\ 0.00014 & 0.00033 & 0.9996 & 2.3996 \\ -0.00000 & 0.00014 & -0.00035 & 0.9996 \end{bmatrix}$$

module $B_0 = 1.458$ T

M4

$$\begin{bmatrix} 0.9967 & 2.397 & -0.00102 & -0.00247 \\ -0.00269 & 0.9967 & 0.000002 & -0.00102 \\ 0.00102 & 0.00247 & 0.9967 & 2.397 \\ -0.000002 & 0.00102 & -0.00269 & 0.9967 \end{bmatrix}$$

module $B_0 = 4$ T

The matrix for the full snake can be obtained by matrix multiplication of the modules M_1 and M_4, separated by a drift matrix D of 0.32m, the design distance between modules, i.e.:

$$\Sigma = M_1 \otimes D \otimes M_4 \otimes D \otimes M_4 \otimes D \otimes M_1$$

The resulting snake matrix Σ at $\gamma = 27$ is:

$$\begin{bmatrix} 0.9659 & 10.7248 & -0.00225 & -0.02500 \\ -0.00606 & 0.9679 & 0.000014 & -0.00225 \\ 0.00225 & 0.02500 & 0.9659 & 10.7248 \\ -0.000014 & 0.00225 & -0.00606 & 0.9679 \end{bmatrix}$$

4. The one turn map

The model to obtain a linear representation of the ring (1-turn map) is simply to place the snakes and rotators in their lattice position, project snakes and rotators and connect their respective ring locations by a phase space rotation: the 1-turn matrix T is obtained by multiplication of the matrices representing these operations (See Figure 6).

Figure 6. Model for the 1-turn matrix

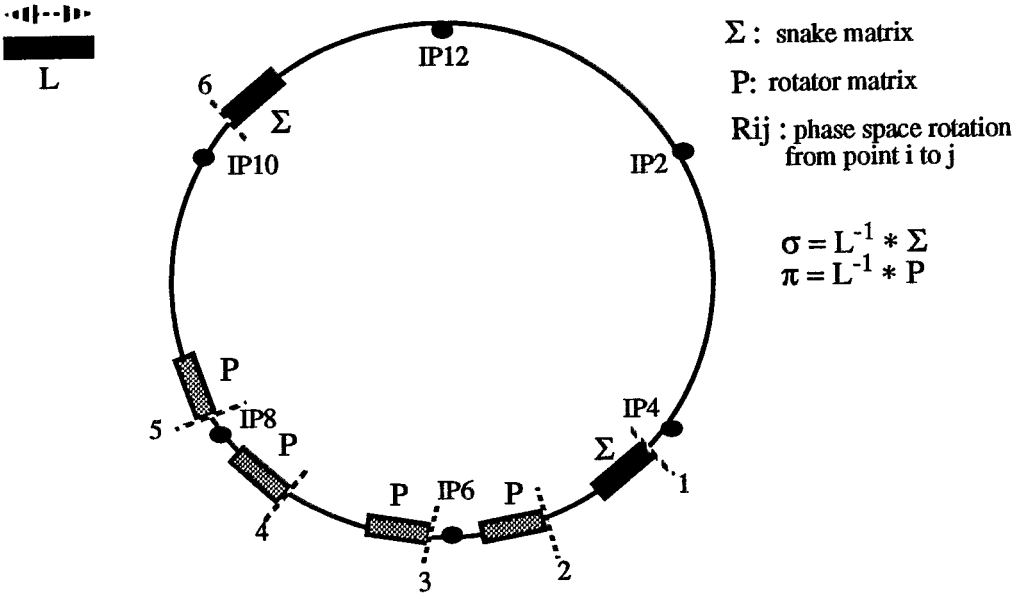

$$T = R_{61} * \sigma * R_{56} * \pi * R_{45} * \pi * R_{34} * \pi * R_{23} * \pi * R_{12} * \sigma$$

The phase space rotation between point *i* and *j* is given by:

$$\begin{bmatrix} R_{ij}^{x} & 0 \\ 0 & R_{ij}^{y} \end{bmatrix}$$

where

$$R_{ij} = \begin{bmatrix} \sqrt{\frac{\beta_j}{\beta_i}}(\cos 2\pi\mu_{ij} + \alpha_i \sin 2\pi\mu_{ij}) & \sqrt{\beta_i\beta_j}\sin 2\pi\mu_{ij} \\ -\frac{1+\alpha_i\alpha_j}{\sqrt{\beta_i\beta_j}}\sin 2\pi\mu_{ij} + \frac{\alpha_i - \alpha_j}{\sqrt{\beta_i\beta_j}}\cos 2\pi\mu_{ij} & \sqrt{\frac{\beta_i}{\beta_j}}(\cos 2\pi\mu_{ij} - \alpha_j \sin 2\pi\mu_{ij}) \end{bmatrix}$$

As described in more detail in [1], it is possible to derive from the 1-turn matrix T the linear coupling effect, quantified by the distance of minimum approach of tunes (ΔQ_{min}) in the following

way. By writing the 4x4 matrix T as $\begin{bmatrix} M & m \\ n & N \end{bmatrix}$, one can demonstrate that:

$$[\cos(2\pi Q_A) - \cos(2\pi Q_B)]^2 = \left[\frac{1}{2} Tr(M-N)\right]^2 + detH$$

where $H = m + n^+$ and A and B are the eigenmatrices and Q_A and Q_B the eigentunes of the coupled motion. In the particular case when $Q_x = Q_y = Q_0$ (fractional tunes) one can demonstrate that the minimum tune separation is:

$$\Delta Q_{min} = \frac{1}{2\pi} \frac{\sqrt{detH}}{\sin(2\pi Q_o)}$$

The program that implements the above calculations for the RHIC lattice [12] is available in the Public Area of the RHIC Unix Domain.

5. Results and discussion

When only the 2 Siberian snakes are present in the lattice (tuned at Q_x=28.185, Q_y=29.185) the results for the linear model at injection are summarized in Table 1.

Table 1: Coupling introduced by 2 snakes in the ring (linear models)

model	ΔQ_{min}
2 snakes (analytical snake matrices)	0.00157
2 snakes (numerical 'SNIG' matrices)	0.00289

The first row in Table 1 gives the linear coupling for 2 snakes in the ring, represented by analytical matrices as described in section 3.3. In the second the matrices for the 2 snakes are obtained numerically (see section 3.1). The predictions from the analytical and numerical model are in within a factor 2: it is worth recalling that the approximations used and the fringe field models are different in the 2 cases, so perfect agreement was not expected.
The results concerning the analytical model have been independently verified [13] by inserting the analytical snake matrices in the RHIC lattice and using the code SYNCH to calculate ΔQ_{min}. The results in this case are in within 1% agreement with the results obtained with the 1-turn matrix model.
Table 2 describes the resulting coupling when we add 4 spin rotators to the 2 snakes in the ring at

injection energy (both rotators and snakes described by numerical 'SNIG' matrices).

Table 2:

model	ΔQ_{min}
2 snakes + 4 rotators (no fringe fields)	0.00303
2 snakes + 4 rotators (with fringe fields)	0.00383

The rotators do not add an appreciable amount of linear coupling to the machine; the fringe fields, as already noticed, are important as far as rotator design and performance evaluation are concerned.

For all the models and configuration studied, however, the resulting linear coupling ($\Delta Q_{min} < 10^{-2}$) at injection is well within the range of capability of the RHIC decoupling system. At storage, the coupling introduced by the snakes is negligible ($\Delta Q_{min} < 10^{-4}$).

Work is in progress to evaluate the higher order effects of the snake on the beam dynamics, and the non-linear behavior will have to be compared to the linear effects.

References

[1] S.Peggs, "Coupling and Decoupling in Storage Rings", IEEE Conference-1983-page 2460

[2] A. Luccio, SNIG Program, Private Communication, August 1994

[3] N. Malitsky, "Application of a differential algebra approach to a RHIC helical dipole", RHIC/AP/51

[4] E. Courant, "Orbit matrices for helical snakes", RHIC/AP/47

[5] A.Luccio, Presented at the Spin Acceleration Meeting, BNL, October 6, 1994

[6] V.Ptitsin, "Symmetric designs for helical spin rotators at RHIC", RHIC/AP/49

[7] A.Luccio, Presented at the Spin Acceleration Meeting, BNL, January 26, 1995

[8] A. Luccio, "Field of a helix", 3rd Workshop on Siberian Snakes, BNL-September 1994

[9] J.P.Blewett, R.Chasman, "Orbits and fields in the helical wiggler", Journal of Applied Physics Vol.48, No 7, July 1977

[10] V.Ptitsin, RHIC/AP/41

[11] N.Malitsky, Program HELIX, RHIC Unix Domain (/rap/PAC++)

[12] F.Pilat, Program DQMIN, Rhic Unix Domain (/rap/lattice_tools/dqmin)

[13] E. Courant, Private Communication, October 1994